

Jaw myology and bite force of the monk parakeet (Aves, Psittaciformes)

Julieta Carril,^{1,2} Federico J. Degrange^{2,3} and Claudia P. Tambussi^{2,3}

¹Cátedra de Histología y Embriología Animal, Facultad de Ciencias Naturales y Museo, Universidad Nacional de La Plata, Buenos Aires, Argentina

²Consejo Nacional de Investigaciones Científicas y Técnicas (CONICET), CONICET is a national institution, Argentina

³Centro de Investigaciones en Ciencias de la Tierra (CICTERRA), CONICET-UNC, Córdoba, Argentina

Abstract

Psittaciform birds exhibit novelties in jaw bone structure and musculature that are associated with strong bite forces. These features include an ossified *arcus suborbitalis* and the muscles *ethmomandibularis* and *pseudomasseter*. We analyse the jaw musculature of the monk parakeet (*Myiopsitta monachus*) to enable future studies aimed at understanding craniofacial development, morphology, function and evolution. We estimate bite force based on muscle dissections, physiological cross-sectional area and skull biomechanical modelling. We also compare our results with available data for other birds and traced the evolutionary origin of the three novel diagnostic traits. Our results indicate that, in *Myiopsitta*, (i) the *arcus suborbitalis* is absent and the orbit is ventrally closed by an elongate *processus orbitalis* and a short *ligamentum suborbitale*; (ii) the *ethmomandibularis* muscle is a conspicuous muscle with two bellies, with its origin on the anterior portion of the *septum interorbitale* and insertion on the medial aspect of the mandible; (iii) the *pseudomasseter* muscle consists of some fibers arising from the *m. adductor mandibulae externus superficialis*, covering the lateral surface of the *arcus jugalis* and attaches by an aponeurotic sheet on the *processus orbitalis*; (iv) a well-developed adductor mandibulae complex is present; (v) the bite force estimation relative to body mass is higher than that calculated for other non-psittaciform species; and (vi) character evolution analysis revealed that the absence of the *arcus suborbitalis* and the presence of the *m. pseudomasseter* are the ancestral conditions, and mapping is inconclusive about presence of one or two bellies of the *m. ethmomandibularis*.

Key words: *ethmomandibularis* muscle; evolutionary novelties; *Myiopsitta monachus*; neotropical parrots; physiological cross-sectional area; *pseudomasseter* muscle; skull biomechanics; suborbital arch.

Introduction

The study of jaw muscles is critical for understanding homologies, functional analyses, and head evolution (Zweers et al. 1994; Gussekloo & Bout, 2005a,b; Holliday, 2009). Moreover, functional morphology of the feeding apparatus provides a basis for studying the systematics, ecology and evolution of birds (Bhattacharyya, 2013). Such studies are of particular interest in Psittaciformes (cockatoos and parrots) because they exhibit evolutionary novelties in the anatomy of the jaw and associated musculature (Zusi, 1993; Tokita, 2003, 2004; Tokita et al. 2007).

Psittaciformes skulls are derived among birds, having highly developed cranial kinesis, robust and recurved maxil-

las with large palatines, and broad mandibles (Zusi, 1993). The novel structures of these skulls include the presence of an ossified *arcus suborbitalis* (ASO) and the jaw muscles *ethmomandibularis* (EM) and *pseudomasseter* (PM). While the EM is present in all Psittaciformes for which information is available, the PM and the ASO may be independently present or absent (Zusi, 1993). The ASO is formed by the fusion of the caudal extension of the *processus orbitalis* of the *os lacrimale*, with the *processus postorbitalis* of the *os squamosum* ventrally limiting the orbit (Zusi, 1993; Tokita, 2003). When the ASO is absent, an elongate *processus orbitalis* and a *ligamentum suborbitale* close the orbit (Tokita, 2003; Tokita et al. 2007). The EM is a large muscle derived from the *m. pterygoideus pars dorsalis* (Hofer, 1950, 1953; Burton, 1974; Tokita, 2004), while the PM is a branch of the *m. adductor mandibulae externus* (Lubosch, 1933; Hofer, 1950, 1953; Zusi, 1993; Tokita, 2004). These three evolutionary novelties are associated with Psittaciformes' high bite forces (Burton, 1974; Zusi, 1993; Tokita, 2003, 2004; Bhattacharyya, 2013), enabling them to crack the hard shells of nuts and

Correspondence

Julieta Carril, Calle 64 N°3, La Plata B1900BVA, Buenos Aires, Argentina. T: +54-011-1559520903; E: julyetacarril@gmail.com

Accepted for publication 21 April 2015

Article published online 5 June 2015

seeds to access the highly nutritious contents (Collar, 1997). Psittacids are capable of shelling and/or cutting a food item by placing it between the sharp frontal edge of the mandible and the maxilla grooves while rotating the item with the muscular tongue (Zusi, 1993; Collar, 1997). The beak is also used as a third point of support during arboreal locomotion (Burton, 1974; Carril et al. 2014a).

Studies of jaw musculature in Psittaciformes include old contributions providing general information for a few species (Lakjer, 1926; Lubosch, 1933; Moller, 1950; Gregory, 1951; Dubale & Rawal, 1965). Hofer (1950, 1953) was the first to describe in detail the jaw muscles of several psittacids in a comparative context, with emphasis on the PM, followed by Burton (1974), who focused on the EM. More recent work has centered on describing the jaw muscles of some Neotropical parrots (Porto, 2004), and elucidating the development of cockatiel *Nymphicus hollandicus* jaw muscle novelties (Tokita, 2004, 2006; Tokita et al. 2013).

Previous theoretical functional inferences about Psittaciformes strong bite force-generating capabilities have been made based only on jaw muscles descriptions (Burton, 1974; Zusi, 1993; Tokita, 2003, 2004; Bhattacharyya, 2013), but there is no empirical data to support them. Here, we address the lack of knowledge in this field by taking a multi-faceted approach to estimating bite force, using skull biomechanics and physiological cross-sectional area measurements in addition to a detailed description of the jaw muscles. We apply this approach to the monk parakeet (*Myiopsitta monachus*; Boddaert, 1783) with the idea of forming a baseline from which to compare with other birds. The monk parakeet is one of the few Neotropical species whose capture has no restrictions due to its pest status (Canavelli et al. 2013), providing benefits for the abundant availability of specimens. This study represents the first description of the jaw musculature for the monk parakeet and the first estimate of bite force for a psittacid. We expected to find that, as described for other Psittaciformes, the jaw adductor muscles would be larger relative to body mass and together with the novel traits, will allow the generation of higher bite forces in the monk parakeet compared with non-Psittaciformes from which data is available. We also verify the presence of the ASO, the EM and the PM in *Myiopsitta*, and trace the evolution of these three diagnostic traits commonly used for taxonomic classification over a combined molecular phylogeny to infer the characteristics at ancestral nodes.

Methods

Dissected specimens and character mapping

Eight adult specimens of the monk parakeet *Myiopsitta monachus* from La Plata (Buenos Aires) and Deán Funes (Córdoba), Argentina were caught from the wild and sacrificed by cervical dislocation (according to protocols approved by the animal care committee and adhered to the legal requirements of Argentina), fixed by

immersion in a 4% formaldehyde solution for 48 h, preserved in 70% alcohol, and dissected under a stereomicroscope Leica S6D. The morphology of jaw muscles and tendons was studied using an iodine staining technique (Bock & Shear, 1972) to enhance visibility. The muscles were identified and removed carefully from their origin and insertion sites. The descriptions follow the order of appearance from superficial to deep muscles. Photos of the muscles were taken with a Nikon D-40 digital camera. The osteological nomenclature follows Baumel & Witmer (1993), and the myological nomenclature follows Holliday & Witmer (2007). The function of each muscle is given by Bhattacharyya (2013).

We traced the evolution of three diagnostic traits (the presence of the *arcus suborbitalis*, the presence of the *m. pseudomasseter* and the number of bellies of the *m. ethmomandibularis*) over a combined molecular phylogeny using parsimony (characters states unordered) and Maximum Likelihood (Markov-K-state1, with equal probability for any particular character change) approaches. Analyses were conducted in Mesquite Version 3.01 (Maddison & Maddison, 2014). Information on the studied characters was retrieved from the literature (Hofer, 1950, 1953; Zusi, 1993; Tokita, 2003, 2004; Porto, 2004; Carril et al. 2014b) and from our own observations in *Myiopsitta*. The tree used is based on the combination of phylogenies of Tavares et al. (2006) and Wright et al. (2008).

Biomechanical modelling

In order to estimate the magnitudes of the forces exerted at the level of the jaws, we used a biomechanical model following Sustaíta (2008). Although many factors contribute to the production of bite forces (e.g., the arrangement of bones, cranial kinesis, ligaments, external and internal forces acting on the bill, rhamphotheca; Bock, 1964), we modeled the mandible in isolation in order to estimate the contribution of the adductor muscle to the force of the jaw. We included only the adductor muscles with insertion on the lower jaw in the model (Ptv, Ptd, EM, Pss, AMEp, AMEs + PM and AMP). The skull can be considered as a system of lever arms with the pivot (fulcrum) at the quadrate-mandibular joint (Bock, 1964, 1974; Fig. 1). It can be considered as a third order lever (i.e., the input-force is between the fulcrum and the output-force). In our model, the input-force is generated by the muscle contraction and the output-force is the one that acts upon the food item at the most rostral bill tip (i.e. initial point of food contact and also crushing point in *Myiopsitta*) in order to have uniformity in data acquisition for subsequent comparisons (Fig. 1). The in-lever moment arm is measured as the perpendicular distance measured between the pivot and the lines of each jaw muscle action, whereas the out-lever moment arm is the straight length from the pivot to the distal end of the bony mandible (Fig. 1 and 2). Moment arm measurements were taken in two ways, with the beak closed and opened to the maximum gape (Fig. 2), measuring from our own videos and photos from live captive specimens taking different food items from the ground. Because the actual lines of action of some muscles are often hard to estimate as they have a large area of origin and/or insertion (e.g., *m. adductor mandibulae externus superficialis* and *mm. pterygoideus*), we followed the proposal of Vizcaino et al. (1998) which allows through a geometric method to obtain values of moment arms regardless of the line of action. This methodology is adequate to apply in dissected and dry skulls. According to this, two lines between the most anterior and posterior part of the insertion and the center of the origin are drawn (Fig. 2). This center is calculated by establishing two

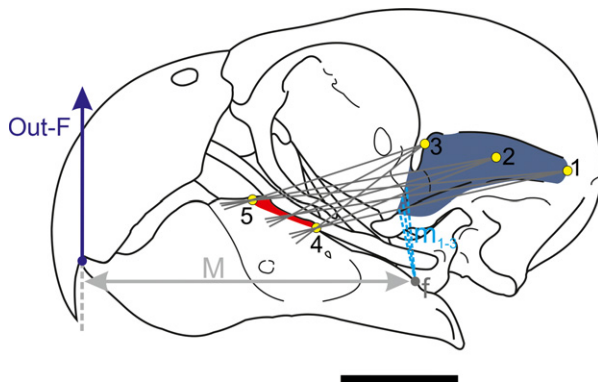


Fig. 1 Biomechanical modelling of the jaw in *Myiopsitta monachus*. Two lines between the most anterior (5) and posterior (4) part of the insertion and the most posterior (1), center (2) and most anterior part (3) of the origin are drawn. The angle between the two lines is subdivided into several lines of action. All the moment arms (m_{1-3}) are measured for each point (posterior, center and anterior) and a mean moment arm is estimated for each point. With the three moments arms, a mean moment arm is calculated. The procedure is then repeated for other muscles (input-force). See text for further explanation. Abbreviations: 1–3, most posterior, center and anterior points of the muscle origin; 4–5, most posterior and anterior edges of muscle insertion; f, fulcrum; m_{1-3} , in-lever moment arms for the three lines between points 1 and 4 and 5; M, out-lever moment arm; out-F, output force. Scale = 1 cm.

peripheral points in the muscle origin (the most antero-dorsal and postero-ventral sites), and the midpoint between them is estimated (Vizcaíno et al. 1998; Fig. 2). The angle between the two lines is subdivided into several lines of action (although Vizcaíno et al. 1998 does not recommend more than five). All the moment arms are measured and a mean moment arm is estimated. This procedure is repeated but changing the point of origin to the most posterior and most anterior point. With the three moments arms (posterior, middle and anterior), a mean moment arm is calculated, which represents the moment arm for the line of action of the studied muscle. The procedure is then repeated for any other muscle (jaw muscles in this case). The mechanical advantage (MA) of bone-muscle lever systems can be expressed as the ratio between the in-lever arm and the out-lever arm (Hildebrand & Goslow, 2001). Since most birds are isognathous (i.e., bites at the same time on both sides; Witmer & Rose, 1991), the analysis can be applied to each side. The cranio-mandibular joint was considered frictionless and the actions of the ligaments were dismissed (Sustaita, 2008).

Physiological cross-sectional area (PCSA)

To calculate theoretical bite force, the PCSA of each muscle was calculated following Sustaita (2008). The PCSA was estimated as the muscle mass multiplied by the cosine of the average angle of pinnation, divided by the density of muscle tissue (1060 kg m^{-3} ; Pennycuik, 1996) multiplied by the average fascicle length (Sustaita, 2008). After being dissected, each muscle was weighed with a digital balance (0.001 g precision). All the muscles were bipinnate, so fascicle angles were measured relative to the axis of the central muscle tendon. Muscles were immersed in 15% HNO_3 for 24 h in order to dissolve the connective tissue that binds the fascicles and measure

their length (Sustaita, 2008). The average angle of pinnation and the average fascicle length were obtained from 10 to 20 fibers of each muscle depending on muscles size. Measurements were obtained from digital photographs with a reference grid using Corel DRAW X5 software. Since it is difficult to preserve the integrity of individual muscles during the process of muscle dissection, the PCSA could be calculated in only three of the eight adult specimens we dissected.

Jaw muscle and bite forces

In a balanced system, the product of the input-force with its respective moment arm is equal to the product of the output-force with its respective moment arm. The moment arm is always perpendicular to the direction of the force. The output-force (F_{out}) of each muscle was calculated by the equation of Hildebrand & Goslow (2001): $F_{\text{out}} = F_{\text{in}} \times m/M$, where m is the in-lever moment arm, M is the out-lever moment arm, and F_{in} is the force of the muscle estimated from its PCSA. Estimations of bite forces were calculated as the resultant of all the output-forces multiplied by two, considering both sides of the jaws and assuming bilateral symmetry (Thomason, 1991; Huber & Motta, 2004). Finally, the bite force estimation relative to body mass was calculated in order to compare data obtained from the monk parakeet with other birds. Because we could not measure the body mass of our specimens, we used the mean measurement of *Myiopsitta* body mass (120 g) obtained by Dunning (2008).

Results

Descriptions of the jaw muscles

M. pseudomasseter (PM)

The PM's origin was aponeurotic on the *processus orbitalis* (Fig. 3A,B; Fig. 4A,B,D). Some fibers were ventrally extended, covering the lateral aspect of the anterior half of the *arcus jugalis*. The PM's insertion was fleshy together with the *m. adductor mandibulae externus superficialis* (Fig. 4F). This muscle elevates the lower jaw.

M. adductor mandibulae externus superficialis (AMEs)

Synonymy: AME *medius* (Hofer, 1950); AME *ventralis* (Burton, 1974; Zusi, 1993; Sustaita, 2008); AME *profundus* (Tokita, 2004). This muscle originated through a strong tendon located at the distal edge of the *processus zygomaticus* (Fig. 3A,B; Fig. 4A,B,D). It was cranio-ventrally extended and had a fleshy insertion on a wide area of the lateral aspect of the lower jaw, anterior to the Ptv insertion (Fig. 4F). This muscle elevates the lower jaw.

M. adductor mandibulae externus profundus (AMEp)

Synonymy: AME *superficialis* (Hofer, 1950; Tokita, 2004); AME *rostralis* (Burton, 1974; Sustaita, 2008). The AMEp's fleshy origin was located on the *fossa temporalis*, on the dorso-lateral and medial edges of the *processus zygomaticus*, and on a small portion of the caudal wall of the orbit, medially to the *processus postorbitalis* (Fig. 3A,B; Fig. 4A,B,

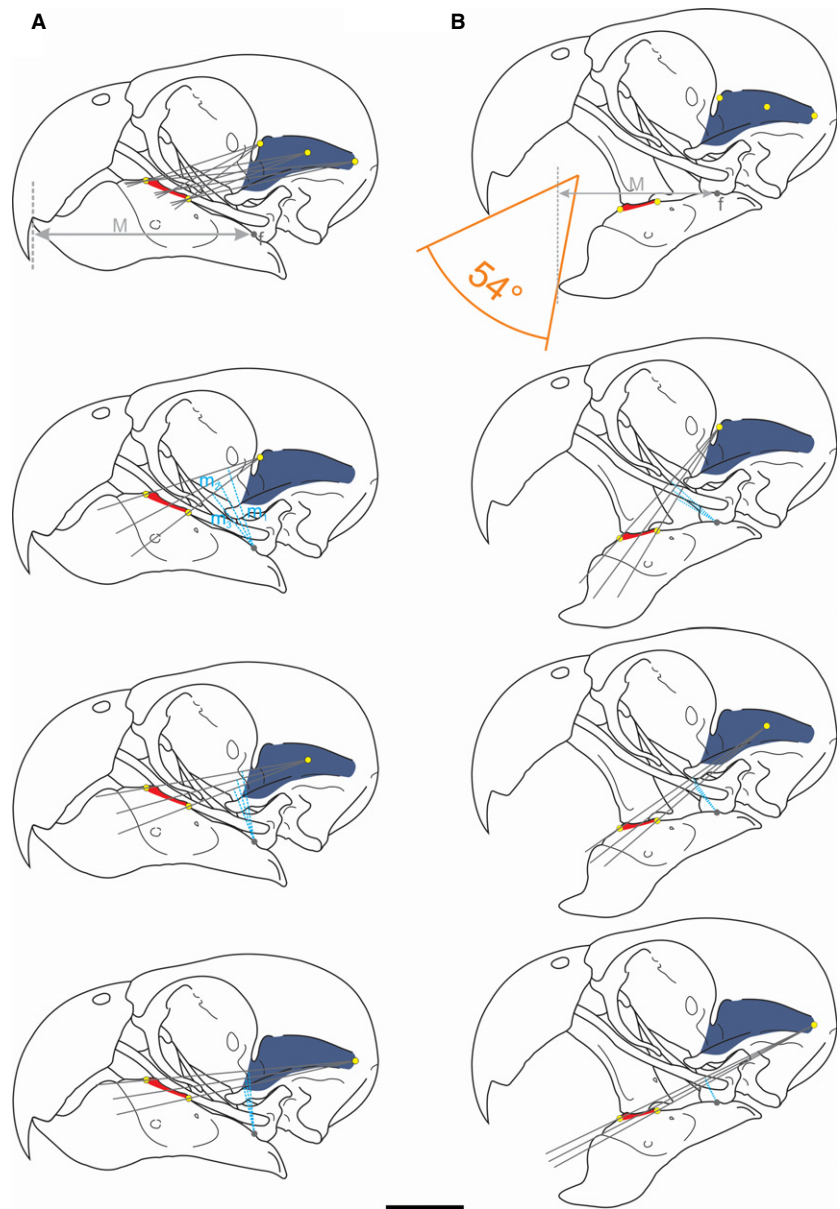


Fig. 2 Moment arms of the *m. adductor mandibulae externus profundus* based on the methodology of Vizcaíno et al. (1998). A, closed beak; B, open beak. Abbreviations: m1-3, in-lever moment arm; M, out-lever. Scale bar = 1 cm. See the text for further information.

D). The AMEp was extended cranio-ventrally and inserted with a tendon on the *processus coronoideus* of the lower jaw, as well as with a fleshy caudal insertion (Fig. 4F). This muscle elevates the lower jaw.

M. adductor mandibulae externus medialis (AMEm)

The AMEm was indistinguishable both anatomically and topologically from AMEp and AMEs.

M. adductor mandibulae posterior (AMP)

This muscle had a fleshy origin on the lateral aspect of the *os quadratum*, anteriorly to the *cotyla quadratojugalis* (Fig. 3E; Fig. 4B,H). It was extended cranio-ventrally. The AMP's insertion was fleshy and tendinous on the medial surface of the lower jaw, dorsal to the Ptd insertion and

caudal to the Pss insertion (Fig. 4E). This muscle elevates the lower jaw.

M. pseudotemporalis superficialis (Pss)

The Pss originated on the *area muscularis aspera* of the orbit (*os laterosphenoidale*) (Fig. 3C–E; Fig. 4A,D). It was ventro-anteriorly projected and inserted on the medial aspect of the lower jaw, anteriorly to the Ptd and AMP insertions and cranio-dorsally to the *fenestra rostralis mandibulae* (Fig. 4E). When the Pss is contracted, the lower jaw elevates.

M. tensor periorbitae (TP)

This lamina muscle was located medially to the *m. pseudotemporalis superficialis* (Fig. 3C). The TP had a wide belly, a

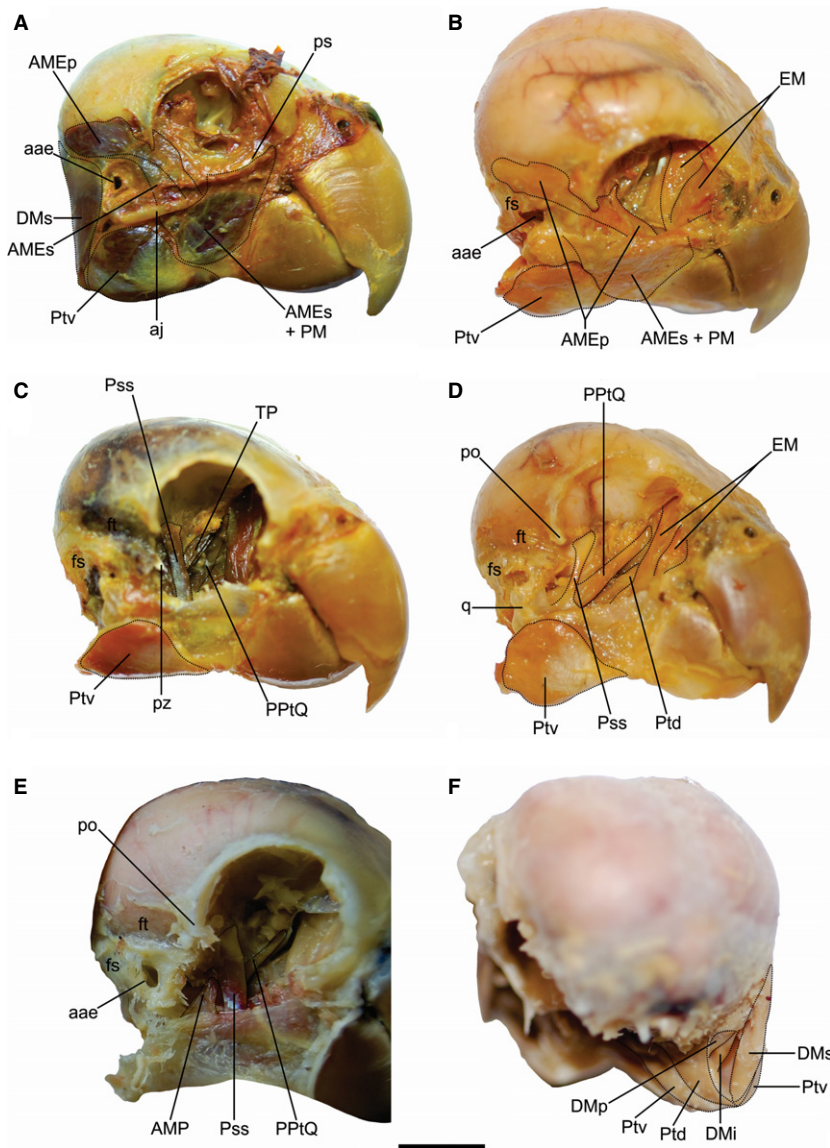


Fig. 3 Jaw muscles of *Myiopsitta monachus*. A, C, D, lateral; B, dorso-lateral; E, cranio-lateral and F, caudal views of the skull. Abbreviations: aae, apertura auris externae; aj, arcus jugalis; AMEp, *m. adductor mandibulae externus profundus*; AMEs, *m. adductor mandibulae externus superficialis*; AMP, *m. adductor mandibulae posterior*; DMi, *m. depressor mandibulae pars intermedia*; DMp, *m. depressor mandibulae pars profunda*; DMs, *m. depressor mandibulae pars superficialis*; EM, *m. ethmomandibularis*; fs, fossa subtemporalis; ft, fossa temporalis; po, processus postorbitalis; PM, *m. pseudomasseter*; PPTQ, *m. protractor pterygoideus et quadrati*; ps, processus orbitalis; Pss, *m. pseudotemporalis superficialis*; Ptd, *m. pterygoideus dorsalis*; Ptv, *m. pterygoideus ventralis*; pz, processus zygomaticus; q, os quadratum. Scale bar = 1 cm.

fleshy origin in the caudo-dorsal portion of the orbit, and a fleshy insertion located caudally to the *foramen opticum* (Fig. 4A,D). This muscle separates the eye from the adductor chamber.

M. pseudotemporalis profundus (Psp)

This muscle was absent in *Myiopsitta monachus*.

M. protractor pterygoideus et quadrati (PPTQ)

The PPTQ exhibited two bellies (Fig. 3C–E) with a fleshy origin at the caudo-ventral portion of the *septum interorbitale* (Fig. 4A,C,D). Both bellies were continued ventro-laterally, and both had fleshy and tendinous insertions on the medial surface of the *os quadratum*, on the *processus mandibularis* and *orbitalis* (Fig. 4G), and on the medial aspect of the proximal region of the *os pterygoideum*. The contraction of this muscle rotates the *os quadratum* anteriorly, pushing

the *os pterygoidei*, the *os palatinum* and the *arcus jugalis* forward, and thus allowing the elevation of the upper jaw.

M. ethmomandibularis (EM)

This was a large muscle with two bellies (Fig. 3B,D). Its single origin was fleshy and was placed on the cranio-dorsal portion of the orbit, on the ethmoidal region (Fig. 4A,B). The EM's single insertion was both fleshy and through a strong tendon on a tubercle located in the medial aspect of the lower jaw, anteriorly to the *fenestra rostralis mandibulae* (Fig. 4E). Its contraction elevates the lower jaw.

M. pterygoideus dorsalis (Ptd)

The Ptd was a large muscle (Fig. 3D,F) whose fleshy origin was on the dorsal aspect of the *os palatinum* and *os pterygoideum* (Fig. 4A,B,D). This muscle was ventro-caudally

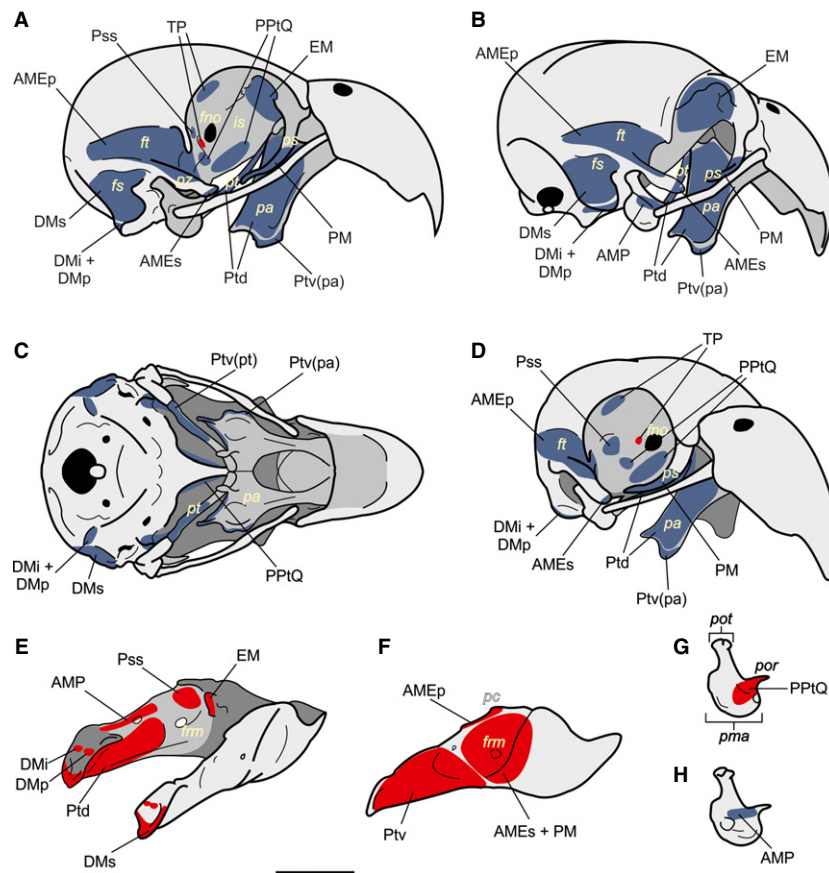


Fig. 4 Cranium and mandible scheme of *Myiopsitta monachus*. A–D, Skull; A, lateral; B, latero-caudal; C, ventral and D, cranio-lateral views. E–F, Jaw; E, detail of the medial aspect of the jaw; F, lateral view. GH, detail of the os quadratum in medial (G) and lateral (H) views. Origins are indicated in blue and insertions in red. Abbreviations: AMEp, *m. adductor mandibulae externus profundus*; AMEs, *m. adductor mandibulae externus superficialis*; AMP, *m. adductor mandibulae posterior*; DMi, *m. depressor mandibulae pars intermedia*; DMp, *m. depressor mandibulae pars profunda*; DMs, *m. depressor mandibulae pars superficialis*; EM, *m. ethmomandibularis*; fno, *foramen nervi optici*; frm, *fenestra rostral mandibulae*; fs, *fossa subtemporalis*; ft, *fossa temporalis*; is, *septum interorbitale*; pa, *os palatinum*; pc, *processus coronoideus*; PM, *m. pseudomasseter*; pma, *processus mandibularis*; pol, *processus orbitalis os lacrimale*; poq, *processus orbitalis os quadratum*; pot, *processus oticus*; PPTQ, *m. protractor pterygoideus et quadrati*; Pss, *m. pseudotemporalis superficialis*; pt, *os pterygoideum*; Ptd, *m. pterygoideus dorsalis*; Ptv(pa), *m. pterygoideus ventralis pars palatina*; Ptv(pt), *m. pterygoideus ventralis pars pterygoidea*; pz, *processus zygomaticus*. Scale bar = 1 cm.

projected, dorsally covering the Ptv. The Ptd's insertion on the lower jaw was fleshy, on the medial aspect of the caudal half and in the ventral portion of the articular zone, on a wide oval-shape fossa (Fig. 4E).

M. pterygoideus ventralis (Ptv)

The Ptv was a conspicuous muscle (Fig. 3A–D,F) consisting of two parts, the *pars palatina* and the *pars pterygoidea*. The *pars palatina* has fleshy and tendinous origins on the distal portion of the *os palatinum* (Fig. 4A–D), while the *pars pterygoidea* has a fleshy origin on the ventral aspect of the *os pterygoideum*, located medially to the PPTQ insertion and ventrally to the *apertura auris externae* (Fig. 4C). The Ptv was projected ventro-caudally, passing towards the ventro-lateral aspect of the lower jaw. Its insertion was fleshy on the caudo-lateral face of the lower jaw (Fig. 4F). The Ptv's ventral portion was partially covered by the *m.*

stylohyoideus and *m. serpihyoideus* of the tongue. Both the Ptd and the Ptv elevate the lower jaw and depress the upper jaw simultaneously.

M. depressor mandibulae (DM)

This muscle can be subdivided into three parts (Fig. 3A,F). The *pars superficialis* (DMs) had fleshy and tendinous origins on the caudo-lateral portion of the occipital region of the skull, on the *fossa subtemporalis* and over the lateral aspect of the *processus paraoccipitalis* (Fig. 4A–C). The DMs was ventrally projected and had a fleshy insertion on the *fossa caudalis* (Fig. 4E). The *pars intermedia* (DMi) and *profunda* (DMp) correspond to two, dorsally fused bellies that originated through an aponeurosis on the *processus paraoccipitalis*, anteriorly to the DMs origin (Fig. 4A–D). Both bellies were inserted fleshily but independently on the most anterior portion of the *fossa*

caudalis, one beside the other (Fig. 4E). The DM depresses the mandible, acting conjointly with the PPTQ in the opening of the jaws.

Biomechanical Modelling, PCSA and Bite Force

Mean muscle masses, PCSA, input-forces, output-forces and the mechanical advantage from the biomechanical modelling for each jaw muscle at closed and maximum opened gape angles (Fig. 2) are presented in Table 1. Total average jaw adductor muscle mass was 1.584 g, while jaw depressor muscle mass was 0.196 g. Combined, the adductor and depressor muscle masses represented 1.483% of the mean body mass. PCSA values calculated ranged from 4.543 mm² for the PPTQ to 24.156 mm² for the Ptv(pa). The Ptv input-force was the highest, almost double that of the Ptd and EM (the second strongest muscle) and triple that of the AMEp and AMEs. MA values differed according to the opening angle of the jaws, and were greater with the beak closed. Thus, calculated output-force values also varied in proportion and were lower at the maximum gape angle for all muscles. Estimated bite force was 12.98 N with the maximum gape angle and 16.74 N with jaws closed.

Ancestral state reconstruction of evolutionary novelties

The reconstruction yielded no conflicts between parsimony and likelihood models, so only results using the parsimony model are shown (Fig. 5).

The reconstruction of character evolution revealed that the absence of the *arcus suborbitalis* (Fig. 5A) was the ancestral condition. This state was preserved in 50% of the species included in the analysis and showed high heterogeneous distribution. Cacatuidae (*Cacatua* + *Probosciger* + *Nymphicus*) changed to the derivative status; while the group formed by *Aprosmictus* + *Electus* + *Tanygnathus* retained the ancestral condition. Within Neotropical parrots, the phylogenetic position of *Amazona* implied that the presence of the *arcus suborbitalis* evolved twice and showed a reversal in *Nandayus*.

According to the reconstruction of Mesquite, the *m. pseudomasseter* could have a single evolutionary origin and its presence was the ancestral condition (Fig. 5B). This status was maintained in 62% of species and no reversals occurred. Among Neotropical parrots, changes to the derived condition occurred in half of the species.

Concerning the evolution of two bellies (*Ara*, *Anodorhynchus* and *Myiopsitta*) or a single belly (remaining taxa) of the *m. ethmomandibularis*, traced was inconclusive. Among the Neotropical parrots in *Primolius*, *Orthopsittaca*, *Aratinga* and *Diopsittaca*, a single belly of the muscle seemed to be the ancestral status.

Discussion

Jaw muscle anatomy and phylogenetic context of skull novelties

The *m. ethmomandibularis* is a parrot-exclusive adductor muscle derived from the *m. pterygoideus dorsalis* (Hofer, 1950, 1953; Burton, 1974; Tokita, 2004). The number of bellies of this muscle differs within the Neotropical parrots (Fig. 5). In *Myiopsitta*, the *m. ethmomandibularis* exhibits two bellies, a condition observed also in *Anodorhynchus* and *Ara* (Porto, 2004); in contrast, *Diopsittaca*, *Orthopsittaca*, *Primolius*, *Aratinga* and *Amazona* exhibit one belly (Porto, 2004).

The *m. pseudomasseter* is embryologically derived from the *adductor mandibulae externus* muscle precursor (Tokita, 2004) and attaches at the *processus orbitalis* or at the *arcus suborbitalis* in many psittacids (Lubosch, 1933; Hofer, 1950, 1953; Zusi, 1993; Tokita, 2004). Our dissections of adult specimens allowed us to affirm that the *m. pseudomasseter* is fused to the *m. adductor mandibulae externus superficialis* and inserted together in the lateral side of the lower jaw. In *Myiopsitta*, the *m. pseudomasseter* consists of some fibers and an aponeurotic sheet passing laterally to the *arcus jugalis* and attaching on the elongated *processus orbitalis*. In contrast, in other taxa such as *Pionites*, *Cacatua*, *Probosciger* and *Nymphicus*, the *m. pseudomasseter* is a noticeable and large muscle with the attachment cranially and/or caudally extended in relation to the *m. adductor mandibulae externus superficialis* (Hofer, 1950; Zusi, 1993; Tokita et al. 2007).

In *Myiopsitta*, the *arcus suborbitalis* is absent and the orbit is ventrally closed by an elongate *processus orbitalis* and a short *ligamentum suborbitale*. The *arcus suborbitalis* has been considered essential to strengthen the skull against the stress caused by the jaw muscle action (Tokita, 2003), and to provide a muscle attachment site (Zusi, 1993; Tokita, 2003). This arch can also fuse with the *processus zygomaticus*, creating a temporal fenestra and providing an additional muscular insertion site for the *m. pseudomasseter*, as in the cockatoos (i. e. *Cacatua*, *Nymphicus* and *Probosciger*; Hofer, 1950; Zusi, 1993; Tokita et al. 2007), or to the well developed *m. pterygoideus ventralis* in *Cyanoramphus* forming the venter externus (Hofer, 1950; Burton, 1974; Zusi, 1993).

While the *m. ethmomandibularis* is present in all members of Psittaciformes, character mapping shows that the occurrence of the *m. pseudomasseter* and the *arcus suborbitalis* is highly variable within the clade Psittaciformes (Tokita et al. 2007; Fig. 5). For example, some taxa such as *Strigops*, *Diopsittaca*, *Primolius*, *Orthopsittaca* and *Ara* do not have *m. pseudomasseter* despite possessing *arcus suborbitalis* (Hofer, 1950, 1953; Zusi, 1993), while in *Pionites*, *Lorius*, *Electus*, *Chalcopsitta*, *Platycercus* and *Agapornis*, the *arcus*

Table 1 Variables of the jaw muscle of *Myiopsitta monachus*.

| Jaw muscle | M ± SE | PCSA | F _{in} | MA _{0°} | MA _{54°} | F _{out 0°} | F _{out 54°} |
|------------|---------------|--------|-----------------|------------------|-------------------|---------------------|----------------------|
| TP | 0.014* | – | – | – | – | – | – |
| PPtQ | 0.031 ± 0.011 | 4.543 | 1.136 | – | – | – | – |
| Ptv(pa) | 0.135 ± 0.010 | 24.156 | 10.167 | 0.146 | 0.123 | 1.483 | 1.251 |
| Ptv(pt) | 0.119 ± 0.024 | 16.512 | – | – | – | – | – |
| Ptd | 0.150 ± 0.014 | 23.118 | 5.780 | 0.174 | 0.159 | 1.007 | 0.918 |
| EM | 0.152 ± 0.018 | 21.812 | 5.453 | 0.515 | 0.370 | 2.811 | 2.019 |
| Pss | 0.042 ± 0.002 | 9.324 | 2.331 | 0.370 | 0.255 | 0.862 | 0.595 |
| AMEp | 0.090 ± 0.006 | 14.321 | 3.580 | 0.294 | 0.174 | 1.053 | 0.624 |
| AMEs + PM | 0.075 ± 0.014 | 14.464 | 3.616 | 0.291 | 0.272 | 1.053 | 0.985 |
| AMP | 0.029 ± 0.008 | 7.399 | 1.850 | 0.056 | 0.055 | 0.103 | 0.101 |
| DMs | 0.084 ± 0.016 | 9.254 | 2.314 | – | – | – | – |
| DMi + DMp | 0.014 ± 0.006 | – | – | – | – | – | – |

*Mass value for only one muscle measured.

AMEp, *m. adductor mandibulae externus profundus*; AMEs, *m. adductor mandibulae externus superficialis*; AMP, *m. adductor mandibulae posterior*; DMi, *m. depressor mandibulae pars intermedia*; DMp, *m. depressor mandibulae pars profunda*; DMs, *m. depressor mandibulae pars superficialis*; EM, *m. ethmomandibularis*; F_{in}, input-forces (in Newtons); F_{out}, output-forces (in Newtons) calculated by the multiplication of F_{in} with MA 0° (beak closed) and 54° (maximum gape angle); MA, mechanical advantage (the ratio between the in-lever arm and the out-lever arm); M, muscle mean mass (in grams); PCSA, physiological cross-sectional area (in mm²); PM, *m. pseudomasseter*; PPtQ, *m. protractor pterygoideus et quadrati*; Pss, *m. pseudotemporalis superficialis*; Ptd, *m. pterygoideus dorsalis*; Ptv(pa), *m. pterygoideus ventralis pars palatina*; Ptv(pt), *m. pterygoideus ventralis pars pterygoidea*; SE, standard error (df: n-1).

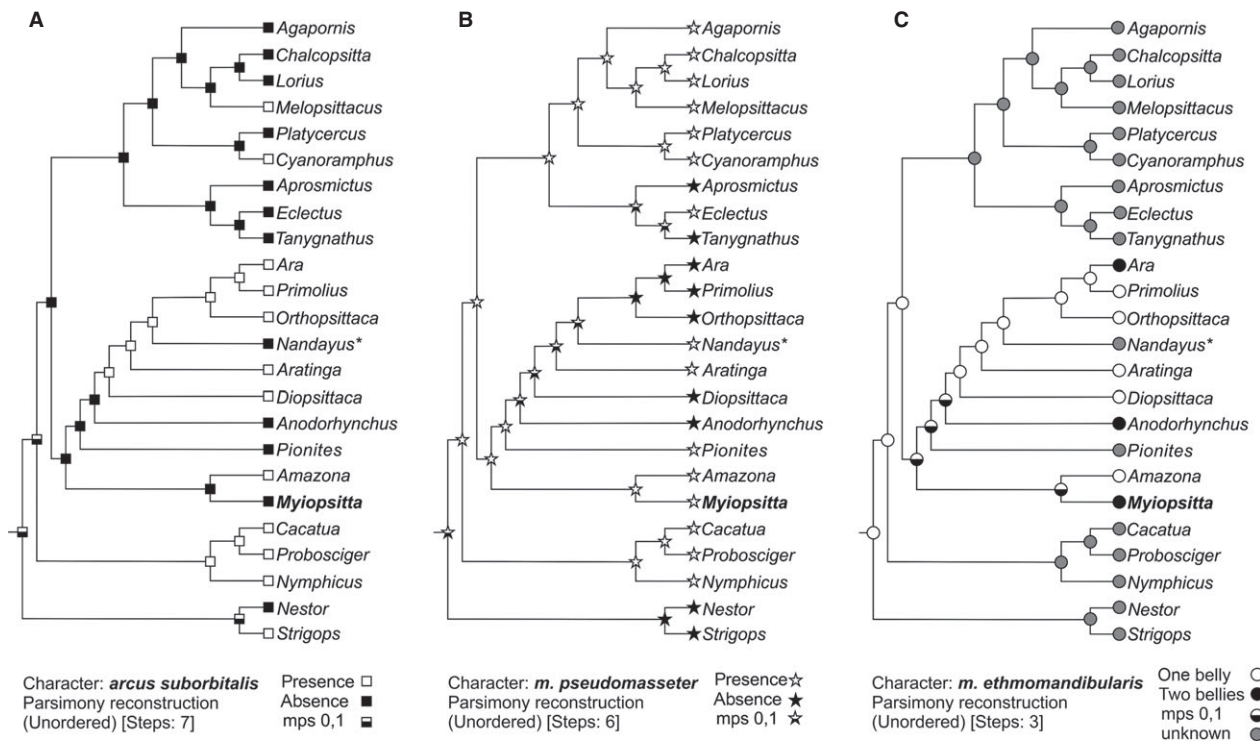


Fig. 5 Ancestral-state reconstructions of (A) *arcus suborbitalis*, (B) *m. pseudomasseter* and, (C) *m. ethmomandibularis* in Psittaciformes based on Parsimony analysis. Phylogenetic proposal modified from Tavares et al. (2006) and Wright et al. (2008). mps, most parsimony state; *data of the extinct *Nandayus vorohuensis* obtained from Carril et al. (2014b).

suborbitalis is absent and the *m. pseudomasseter* is present (Hofer, 1950, 1953; Zusi, 1993; Tokita et al. 2007), a situation also inferred in the extinct Pliocene species *Nandayus*

vorohuensis (Tonni & Noriega, 1996; Carril et al. 2014b) and shared with *Myiopsitta*. Both the *arcus suborbitalis* and *m. pseudomasseter* are present in *Amazona*, *Aratinga*,

Cyanoramphus, *Melopsittacus* and in all members of the Australasian Family Cacatuidae (Hofer, 1950, 1953; Zusi, 1993; Tokita, 2003, 2004; Tokita et al. 2007), and both are absent in *Nestor*, *Tanygnathus*, *Aprosmictus* and *Anodorhynchus* (Hofer, 1950, 1953; Zusi, 1993; Porto, 2004).

It has been postulated that the *arcus suborbitalis* and the *m. pseudomasseter* work as an integrated morphological and functional system (Zusi, 1993). However, character mapping analyses by Tokita et al. (2007) showed that they are independent or decoupled units and evidence their recurrence caused by modularity and/or heterochrony in development. Here, we added new character state information for the *arcus suborbitalis* and the *m. pseudomasseter* in *Myiopsitta*, and included Neotropical species studied by Porto (2004) in a phylogenetic analysis. Ancestral state reconstruction reveals independent evolution of *arcus suborbitalis*, and its absence as the ancestral condition. Interestingly, ossified suborbital arch acquisition occurs in the adult stage by subocular ligament ossification (Tokita, 2004). We hypothesize that this process (ossification during ontogeny) may be a mechanism of origin of this phenotypic novelty but is not possible to elucidate if this convergent trait is adaptive. Reconstruction of the character history of the *m. pseudomasseter* presence revealed a single evolutionary origin and the derived condition (its absence) arose multiple times. The potential advantages of either state are difficult to discern but it is suitable to infer that the presence of this muscle may have functional advantages. This of course, is not linear and depends on many other variables such as the amount and form of fibers as were already mentioned.

Regarding other jaw muscles, the *m. protractor pterygoideus et quadrati* has a double origin in *Myiopsitta*, whereas *Anodorhynchus* shows a triple origin of this muscle (Porto, 2004). The *m. pseudotemporalis profundus* is absent in *Myiopsitta* as well as in all the Psittaciformes for which the mandibular musculature is known (Hofer, 1950, 1953; Burton, 1974; Porto, 2004). Finally, in some parrots such as *Cyanoramphus* and *Platyercus*, but not in *Myiopsitta*, the *m. depressor mandibulae* expands cranially, occupying the external auditory meatus (Zusi, 1993).

Functional morphology and force-generating capacity

In birds, the opening of the jaws is the result of the action of two muscles, the *m. protractor pterygoideus et quadrati*, which elevates the upper jaw, and the *m. depressor mandibulae*, which depresses the mandible (Bock, 1964). The protractor muscle of the quadrate is poorly developed and scored the lowest PCSA values when compared to the other jaw muscles (Table 1). On the other hand, the mass of the *m. depressor mandibulae* is considerable, although its PCSA is among the lowest values (Table 1). This lack of concordance between muscle mass and PCSA value could be

because the primary function of this muscle is to depress the jaw. This explanation is congruent with Zusi's (1993) finding that parrots are not among the bird lineages that have evolved a jaw system for powerful beak opening.

The closing of the bill is accomplished by the action of various muscles which act together to elevate the lower jaw and to depress the upper jaw. In *Myiopsitta monachus*, the *m. adductor mandibulae externus* complex, the *m. pterygoideus* as well as the *m. ethmomandibularis* are highly conspicuous muscles, providing a strong jaw adduction which directs the lower jaw upward, allowing them to feed on seeds, nuts, thistles, herbs, fruits, leaf buds, blossoms and insects (Collar, 1997).

The PCSA is a direct estimate of the force-generating capacity of a muscle, which in turn relates to its mass, pinnation angle and fascicle length. In our measurements, *m. pterygoideus ventralis*, *m. pterygoideus dorsalis* and *m. ethmomandibularis* muscles achieved the highest PCSA values (Table 1). The fibers of these muscles are short, and their masses and pinnation angle are the highest of the muscles we measured. Also, the mechanical advantage (MA) gives an idea of how much force is needed or how faster a system works. The highest MA values were obtained for *m. ethmomandibularis*, *m. pseudotemporalis superficialis* and *adductor mandibulae externus* muscles (Table 1). Furthermore, the insertion site of the *m. adductor mandibulae externus superficialis* is wider due to the *m. pseudomasseter*, increasing the in-lever moment arm and, thus, the MA and the muscle output-force.

In *Myiopsitta*, the bite force estimation relative to body mass was notably higher (BF/BM = 0.139) than those of other birds, such as raptors, whose beaks are morphologically alike. For example, *Falco peregrinus*, a raptor that tends to kill prey by powerful bites to the neck, has a similar bite force estimation (16.90 N) to *Myiopsitta* (16.74 N), but its body mass is almost six times greater (683.6 g; BF/BM = 0.024; Sustaita, 2008; Table 2). *Accipiter striatus* a hawk that kills its prey by clutching it with its toes and talons has similar body mass (113.5 g) to *Myiopsitta*, but a six times lower bite force estimation value (2.73 N; BF/BM = 0.024; Sustaita, 2008; Table 2).

In vivo bite force data for birds is restricted to a few taxa, mainly Passeriformes (van der Meij & Bout, 2004, 2006; Herrel et al. 2005a,b; Degrange et al. 2010; Soons et al. 2010; Sustaita & Hertel, 2010). Those measurements were obtained using a force transducer. Despite the differences in the methodology, some comparisons can be made with *Myiopsitta*. The maximum bite forces recorded for Estrildidae is 9.60 N for the Java Sparrow *Lonchura oryzivora* (van der Meij & Bout, 2004). For the Fringillidae, the highest value is that of the Collared Grosbeak *Mycerobas affinis* (38.40 N). Strikingly, bite force values for Passeriformes are higher than the bite force calculated for *Myiopsitta*. In other words, smaller birds such as Passeriformes exhibit stronger relative bite forces than *Myiopsitta*. This could be

Table 2 Compared bite force (in Newtons), body mass (in grams) and standardized bite force (BF/BM) of *Myiopsitta monachus* with available published data of raptorial birds and passerines.

| Taxa | Order | BF | BM | BF/BM |
|------------------------------|-----------------|-------|-------|-------|
| <i>Falco sparverius</i> * | Falconiformes | 3.50 | 78.8 | 0.044 |
| <i>Falco mexicanus</i> * | Falconiformes | 16.50 | 487.7 | 0.034 |
| <i>Falco columbarius</i> * | Falconiformes | 5.26 | 137.0 | 0.038 |
| <i>Falco peregrinus</i> * | Falconiformes | 16.90 | 683.6 | 0.024 |
| <i>Accipiter striatus</i> * | Accipitriformes | 2.73 | 113.5 | 0.024 |
| <i>Accipiter cooperii</i> * | Accipitriformes | 3.90 | 342.7 | 0.011 |
| <i>Lonchura oryzivora</i> ** | Passeriformes | 9.60 | 30.4 | 0.315 |
| <i>Mycerobas affinis</i> ** | Passeriformes | 38.40 | 70.0 | 0.548 |
| <i>Myiopsitta monachus</i> | Psittaciformes | 16.74 | 120.0 | 0.139 |

*From Sustaita (2008), using PCSA; **From van der Meij & Bout (2004), using force transducer.

BF, bite force; BM, body mass.

related to the different methodology used to obtain the bite force value and the applied model simplification, and/or to differences in the trophic habit (van der Meij & Bout, 2004, 2006), considering that many passerines eat hard seeds and have less manoeuvrability in their cranio-mandibular complex than do psittacids.

Lastly, it is important to take into account the other factors that can influence bite force, such as the presence of the ramphoteca and the cranial kinesis, which play an important role as a stress dissipative (Bout & Zweers, 2001). In science, most models can not incorporate all the details of a natural complex system. In this paper, we decided to simplify the system modeling the mandible in isolation. This may lead to higher calculated force values for *Myiopsitta* in future studies. We are aware that our interpretations are limited by this simplification but are valid approximations as baseline. Morphology of the bill is also an important factor. Bill safety factors are critical in the evolution of bill morphology (Soons et al. 2010). As in Darwin's finches, the stress resistance of the deep and wide bill of *Myiopsitta* may allow these birds to crack hard food items while limiting the risk of beak failure since they are able to resist higher stress magnitudes (Soons et al. 2010). More complex biomechanical modelling including finite element analysis may shed light on this issue.

Conclusions

The complexity of the jaw musculature of parrots is striking compared with other groups of birds. There are two original components of the mandibular adductor system, both present in *Myiopsitta*: the *m. ethmomandibularis* and *m. pseudomassester*. Additionally, in several Psittaciformes, a new osteological configuration (*arcus suborbitalis*) closes the orbit ventrally, extending the surface for muscles attachment. This bony closure is absent in *Myiopsitta*.

Ancestral state reconstructions and phylogenetic hypothesis indicate that absence of the *arcus suborbitalis* and the presence of the *m.pseudomassester* are the ancestral conditions. However, presence or absence of these traits might not serve as differentiation criterion within psittaciforms. These jaw characters occur heterogeneously in the clade Psittaciformes with diet-habits alike suggesting that they may have evolved repeatedly (Tokita et al. 2007; Carril et al. 2014b). Indeed, the acquisition of these novel characters may have facilitated the diversification of parrot cranial morphology (Tokita et al. 2007).

Several features enable Psittaciformes to exert strong bite forces during feeding and locomotion, including the strong adductor muscles that are evolutionary novelties in this group. However, the presence and/or degree of development of these muscles is variable among different psittaciform species (Burton, 1974; Tokita, 2003, 2004; Bhattacharyya, 2013). Psittaciformes is a species-rich order, and our understanding of the variation in jaw musculature and bite force in this group is limited. However, this deep description of monk parakeet jaw anatomy will serve as a useful reference for phenotypic comparison with other species of parrots as well as future studies of craniofacial development, morphology, function and evolution in psittaciforms and other bird groups.

Acknowledgements

Thanks to the Editor Stefan Milz and two anonymous reviewers for feedback that substantially improved the quality of this paper. Emilia Sferco help us with the mapping characters. The authors are grateful to those who donated specimens to the project including José Picans and Juan José Rustán. We are indebted to Hector Raul Muñoz, Nicolás Quinteros and Ricardo Herrera for their assistance during fieldwork, and to CONICET for its permanent support. We appreciate the improvements in English usage made by Bruce Peterson and Caitlin Stern through the Association of Field Ornithologists' program of editorial assistance.

References

- Baumel JJ, Witmer LM (1993) Osteologia. In: *Handbook of Avian Anatomy: Nomina Anatomica Avium*. (eds Baumel J, King A, Breazile J, Evans H, Vanden BJ), pp. 45–132, No. 23, Massachusetts: Publications of the Nuttall Ornithological Club.
- Bhattacharyya BN (2013) Avian jaw function: adaptation of the seven-muscle system and a review. *Proc Zool Soc* **66**, 75–85.
- Bock WJ (1964) Kinetics of the avian skull. *J Morphol* **114**, 1–41.
- Bock WJ (1974) The avian skeletomuscular system. *Avian Biol* **4**, 119–257.
- Bock WJ, Shear C (1972) A staining method for gross dissection of vertebrate muscles. *Anat Anz* **130**, 222–227.
- Bout RG, Zweers GA (2001) The role of cranial kinesis in birds. *Comp Biochem Physiol A* **131**, 197–205.
- Burton PJK (1974) Jaw and tongue features in Psittaciformes and other orders with special reference to the anatomy of the Tooth-billed pigeon (*Didunculus strigirostris*). *J Zool* **174**, 255–276.

- Carril J, Mosto MC, Picasso MJB, et al. (2014b) Hindlimb myology of the monk parakeet (Aves, Psittaciformes). *J Morphol* **275**, 732–744.
- Carril J, Degrange FJ, Tambussi CP (2014a) Jaw muscle reconstruction of the Late Pliocene Psittaciform *Nandayus vorohuensis* from Argentina. *Ameghiniana* **51**, 361–365.
- Collar NJ (1997) Family Psittacidae (Parrots). In: *Handbook of the Birds of the World, volume 4: Sandgrouse to Cuckoo*. (eds del Hoyo J, Elliott A, Sargatal J), pp. 280–477, Barcelona: Lynx Editions.
- Canavelli SB, Swisher ME, Branch LC (2013) Factors related to farmers' preferences to decrease monk parakeet damage to crops. *Hum Dim Wild* **18**, 124–137.
- Degrange FJ, Tambussi CP, Moreno K, et al. (2010) Mechanical analysis of feeding behavior in the extinct "Terror Bird" *Andalgalornis steulleti* (Gruiformes: Phorusrhacidae). *PLoS ONE* **5**, e11856.
- Dubale MS, Rawal UM (1965) A morphological study of the cranial muscles associated with the feeding habit of *Psittacula krameri* Scopoli. *Pavo* **3**, 1–13.
- Dunning JB (2008) *Handbook of Avian Body Masses*, 2nd edition (ed Dunning JB), pp. 655. Boca Raton, Florida: CRC Press, Taylor & Francis Group.
- Gregory KW (1951) *Evolution Emerging*. pp 736, New York: Macmillan Company.
- Gussekloo SWS, Bout RG (2005a) The kinematics of feeding and drinking in palaeognathous birds in relation to cranial morphology. *J Exp Biol* **208**, 3395–3407.
- Gussekloo SWS, Bout RG (2005b) Cranial kinesis in palaeognathous birds. *J Exp Biol* **208**, 3409–3419.
- Herrel A, Podos J, Huber SK, et al. (2005a) Bite performance and morphology in a population of Darwin's finches: implications for the evolution of beak shape. *Funct Ecol* **19**, 43–48.
- Herrel A, Podos J, Huber SK, et al. (2005b) Evolution of bite force in Darwin's finches: a key role for head width. *J Evol Biol* **18**, 669–675.
- Hildebrand M, Goslow G (2001) *Analysis of Vertebrate Structure*. pp. 635. New York: Wiley.
- Hofer H (1950) Zur Morphologie der Kiefermuskulatur der Vögel. *Zool Jb (Anat)* **70**, 427–556.
- Hofer H (1953) Die Kiefermuskulatur der Papageien des Evolutionsproblem. *Biol Zbl* **72**, 225–233.
- Holliday CM (2009) New insights into dinosaur jaw muscle anatomy. *Anat Rec* **292**, 1246–1265.
- Holliday CM, Witmer LM (2007) Archosaur adductor chamber evolution: integration of musculoskeletal and topological criteria in jaw muscle homology. *J Morphol* **268**, 457–484.
- Huber DR, Motta PJ (2004) Comparative analysis of methods for determining bite force in the Spiny Dogfish *Squalus acanthias*. *J Exp Zool* **301A**, 26–37.
- Lakjer T (1926) *Studien Über Die Trigeminus-Versorgte Kaumuskulatur Der Sauropsiden*. pp. 70, Reitzel, R. A.: Copenhagen.
- Lubosch W (1933) Untersuchungen über die visceralmuskulatur der sauropsiden. *Morph Jb* **72**, 584–666.
- Maddison WP, Maddison DR (2014) *Mesquite: a modular system for evolutionary analysis*, Version 3.01. <http://mesquiteproject.org>
- Moller W (1950) Biologisch-anatomische studien am Schädel von *Ara macao*. *Morph Jah* **70**, 305–342.
- Pennycuik CJ (1996) Stress and strain in the flight muscles as constraints on the evolution of flying animals. *J Biomech* **29**, 577–581.
- Porto M (2004) Anatomia comparada do esqueleto da cabeça e da musculatura da mastigação de *Anodorhynchus Spix*, 1824, *Ara Lacépède*, 1799, *Diopsittaca Ridgway*, 1912, *Prophyrrura Miranda-Ribeiro*, 1920 e *Orthopsittaca Ridgway*, 1912 (Aves: Psittaciformes: Arinae). PhD Thesis, Universidade Federal Rural do Rio de Janeiro. pp. 88.
- Soons J, Herrel A, Genbrugge A, et al. (2010) Mechanical stress, fracture risk and beak evolution in Darwin's ground finches (Geospiza). *Philos Trans R Soc Lond B Biol Sci* **365**, 1093–1098.
- Sustaita D (2008) Musculoskeletal underpinnings to differences in killing behavior between north American accipiters (Falconiformes: Accipitridae) and falcons (Falconidae). *J Morphol* **269**, 283–301.
- Sustaita D, Hertel F (2010) *In vivo bite and grip forces, morphology and prey-killing behavior of North American accipiters (Accipitridae) and falcons (Falconidae)*. *J Exp Biol* **213**, 2617–2628.
- Tavares ES, Baker AJ, Pereira SL, et al. (2006) Phylogenetic relationships and historical biogeography of neotropical parrots (Psittaciformes: Psittacidae: Arini) inferred from mitochondrial and nuclear DNA sequences. *Syst Biol* **55**, 454–470.
- Tokita M (2003) The skull development of parrots with special reference to the emergence of a morphologically unique cranio-facial hinge. *Zool Sci* **20**, 749–758.
- Tokita M (2004) Morphogenesis of parrot jaw muscles: understanding the development of an evolutionary novelty. *J Morphol* **259**, 69–81.
- Tokita M (2006) Cranial neural crest cell migration in cockatiel *Nymphicus hollandicus* (Aves: Psittaciformes). *J Morphol* **267**, 333–340.
- Tokita M, Kiyoshi T, Armstrong KN (2007) Evolution of craniofacial novelty in parrots through developmental modularity and heterochrony. *Evol & Dev* **9**, 590–601.
- Tokita M, Nakayama T, Schneider RA, et al. (2013) Molecular and cellular changes associated with the evolution of novel jaw muscles in parrots. *Proc R Soc B* **280**, 20122319.
- Tonni EP, Noriega J (1996) Una nueva especie de *Nandayus Bonaparte*, 1854 (Aves: Psittaciformes) del Plioceno tardío de Argentina. *Rev. Chil. Hist. Nat.* **69**, 97–104.
- Thomason JJ (1991) Cranial strength in relation to estimated biting forces in some mammals. *Can J Zool* **69**, 2326–2333.
- van der Meij MAA, Bout RG (2004) Scaling of jaw muscle size and maximal bite force in finches. *J Exp Biol* **207**, 2745–2753.
- van der Meij MAA, Bout RG (2006) Seed husking time and maximal bite forces in finches. *J Exp Biol* **209**, 3329–3335.
- Vizcaíno SF, de Iuliis G, Bargo MS (1998) Skull shape, masticatory apparatus, and diet of *Vassallia* and *Holmesina* (Mammalia: Xenarthra: Pamphathiidae). When anatomy constrains destiny. *J Mammal Evol* **5**, 291–322.
- Witmer LM, Rose KD (1991) Biomechanics of the jaw apparatus of the gigantic Eocene bird *Diatryma*: implications for diet and mode of life. *Paleobiology* **17**, 95–120.
- Wright TF, Schirtzinger EE, Matsumoto T, et al. (2008) A multilocus molecular phylogeny of the parrots (Psittaciformes): Support for a Gondwanan origin during the Cretaceous. *Mol Biol Evol* **25**, 2141–2156.
- Zweers GA, Berkhoudt H, Vanden Berge JC (1994) Behavioral mechanisms of avian feeding. In: *Bio-Mechanics of Feeding in Vertebrates. Advances in Comparative And Environmental Physiology*, Vol. 18. (eds Bels VL, Chardon M, Vandewalle P), pp. 241–279, Berlin: Springer-Verlag.
- Zusi RL (1993) Patterns and diversity in the avian skull. In: *The skull: Patterns of Structural and Systematic Diversity*, vol. 2 (eds Hanken J, Hall BK), pp. 391–437. Chicago: University of Chicago Press.